MATERIALS PHYSICS AND MECHANICS RESEARCH ARTICLE

Submitted: February 15, 2025 **Revised: February 23, 2025** **Accepted: June 5, 2025**

Structural and thermal changes in the polyaniline lead sulphide nanocomposite

J.B. Bhaiswar [1]✉, S.P. Dongre [2], D. Meghe [1]

[1] Nagpur Institute of Technology, Nagpur, India

[2] Bhalerao Science College Saoner, India

✉ jitendrabhaiswar@gmail.com

ABSTRACT

In this study, composite films of PbS nanoparticles and PANI were used. The PbS/PANI samples were analyzed using XRD, UV-visible, FT-IR and TEM. Furthermore, the effects of PbSNPs on their optical, structural and thermal parameter were determined using DTA, UV-Visible and XRD. The UV and XRD confirmed the successful synthesis of PbS/PANI Nanocomposite. The TEM indicated homogeneous dispersion of PbS in PANI with average diameter of particle is 20nm. Besides, the broadness and reduction of PANI in XRD peaks intensity with increasing PbS is attributed to the intermolecular interactions of PANI and PbS and indicates the successful incorporation of PbS in PANI. The thermal stability was enhanced at different weight percentages of PbS nanoparticle indicated in DTA analysis. The structural changes in the Pbs nanocomposite observed in the XRD.

KEYWORDS

DTA • thermal analysis • polyaniline • Pbs • TEM • nanocomposite

Citation: Bhaiswar JB, Dongre SP, Meghe D. Structural and thermal changes in the polyaniline lead sulphide nanocomposite. *Materials Physics and Mechanics*. 2025;53(3): 140–148.
http://dx.doi.org/10.18149/MPM.5332025_11

Introduction

Polymer composites are comprehensively used in vehicle, flying, advancement, and electronic applications [1–5]. It was focused on mechanical, electrical, warm and other genuine properties. The nanocomposites are one more class of materials that exhibit superior properties compared to microcomposites [6–9]. A little development of nanoparticles essentially deals with different properties without relinquishing the light weight of polymer lattices. The nanocomposites generally suggest composites in which something like one phase has viewpoint on the solicitation for several nanometers. They can be made with the used of three particular kinds of nanoparticles. The vital sort of nanoparticles simply has one angle in the nanometer scale. They have a platelet-like development [10–14]. Soil is a certifiable delineation of the sort of nanoparticles. Another sort of nanoparticles has two parts of the nanoparticles in the nanometer scale. Nanotubes and nanofibers have a spot with this get-together [15–17]. The third sort of nanoparticles has every one of the three angles in the nanometer scale, for example, round silica particles. A collection of the sort of particles is outstandingly retentive particles. While the component of the particle may be in the solicitation for microns, the pore sizes are in the solicitation for nanometers [18,19].

Publisher: Peter the Great St. Petersburg Polytechnic University

The filling of nanoscopic metals into polymer lattices tends to a decision to course and change issues. For sensible purposes of nanoparticles, polymers are on a very basic level required as filling stage since they would have different qualities: they can be an electrical and warm encasing or conveyor [20]. Polymers could have a hydrophobic or hydrophilic nature and can be definitively hard plastic or flexible versatile, and so on. Ultimately, polymer filling is the least complex and most sensible way for nanostructures metal change, treatment, and application [21–23]. This has fuelled assessment concerning the preparation of metal-polymer nanocomposites. These composites most generally show up as small polymer films or powders, as this is commonly the least demanding development to design, and moreover extraordinary for exploiting the best properties. The Readiness methodologies of polymer metal nanocomposite can be named in-situ and ex-situ procedures. In the in-situ systems, the monomer is polymerized, with metal particles introduced already or after polymerization [24–26]. Then, the metal particles in the polymer structure are reduced falsely, thermally or by UV (ultraviolet) brightening, to shape nanoparticles [27]. In the ex-situ process, the metal nanoparticles are consolidated first, and their surface is normally passivized. In the current paper, Polyaniline/PbS nanocomposite arranged, and it gets examination with DTA (differential thermal analysis) for warm boundary and their solidness.

Materials and Methods

Compound combination of Polyaniline involving APS as oxidant and H_2SO_4 (Fig. 1). Unadulterated aniline broke down in 100 ml refined water with H_2SO_4 added under attractive blending for 2 h. The arrangement of ammonium per sulfate in sulphuric corrosive was then added drop-wise in the arrangement of aniline. The encourage of polyaniline acquired with dim green cloured [28]. The encourage washed with water. A PANI encourage was dried under at 50–100 °C for over 8 h. Blend of PANI/PbS nanocomposites a similar blend process was adjusted for readiness of PANI/PbS nanocomposite at various weight proportion of PbS nanoparticle. PANI nanocomposite was synthetically portrayed by infrared spectroscopy, XRD (X-ray diffraction) and TGA (thermogravimetric analysis).

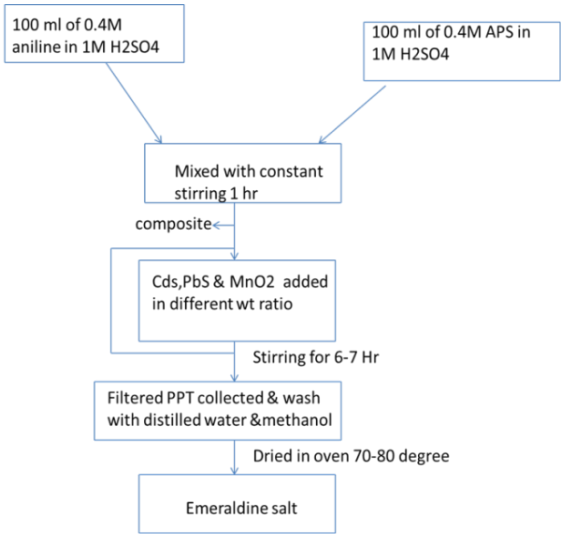

Fig.1. Scheme of synthesis of polyaniline and nanocomposite

Characterization of nanocomposites

XRD with Philips PW-3071, utilizing Cu-Kα radiation of frequency 1.544 Å, with examining pace of 2 °/min at 45 kV and 40 mA. Fourier transform infrared (FTIR) spectroscopy (Perkin Elmer 200) with recurrence of 400-4000 cm^{-1}. Warm examination of test recorded by Perkin-Elmer Precious stone TGA/DTA in argon air at a warming pace of 10 °/min.

XRD characterization of pure PANI and PANI/PbS Nano composite

The XRD patterns of unadulterated PANI and PbS and different wt. % of PANI/PbS nanocomposite are displayed in Figs. 2 and 3. The molecule size of translucent molecule of unadulterated PANI and the nanocomposites are determined by utilizing the Debye-Scherrer equation: $D = 0.94\lambda/\beta\cos\theta$, where D is the typical crystallite size (nm), k is the shape factor, which is much of the time relegated a worth of 0.94, λ is the frequency of Cu Kα radiation (1.5418 Å), β is the full width at half limit of the diffraction top thinking about the revision because of instrumental widening (0.09°). Translucent size of glasslike molecules for unadulterated PANI, unadulterated PbS and different content (wt. %) of PANI/PbS nanocomposite are given in Table 1. From the reference diagram of XRD top plainly as 5–20 wt. % PbS nanoparticle expansions in the PANI lattice the level of crystallites of nanocomposite additionally increments. Unadulterated PANI shows glasslike reflection at explicit point in XRD and undefined at diffused foundation, accordingly it uncovers the polycrystalline construction. It is observed that degree of crystallinity increased in the nanocomposite as compared to pure PANI and PbS, indicated the structural and surface morphological changes in the nanocomposite. Nanocomposite is crystalline and has a more ordered structure compared to pure polyaniline.

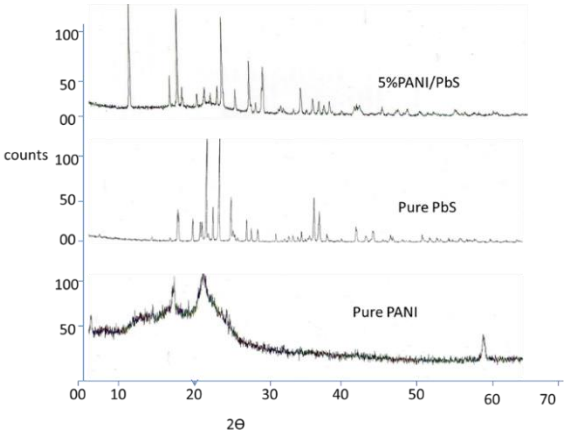

Fig 2. XRD patterns for 5%PANI/PbS nanocomoposite, pure Pbs and PANI

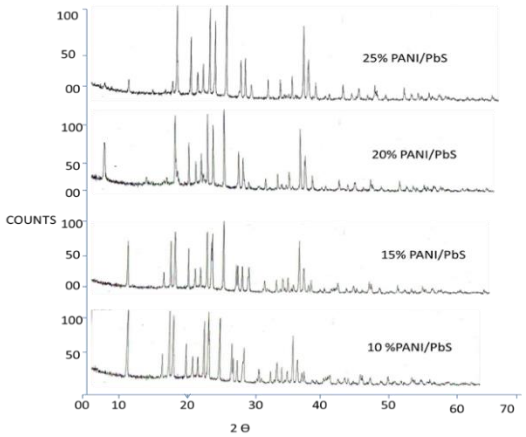

Fig. 3. XRD patterns for PANI/PbS nanocomposites with different contents of PANI

Table.1. Table indicated crystalline size of particle in nanocomposite

Sr. No	Material	Crystalline size particle, nm	D'spacing, Å	2θ, °
1	PURE PANI	0.710	3.520	25.270
2	PURE PbS	0.950	3.210	27.770
3	5% PANI/PbS	1.048	3.230	27.560
4	10% PANI/PbS	1.420	3.240	27.470
5	15% PANI/PbS	1.230	3.012	29.650
6	20% PANI/PbS	1.437	3.009	29.680
7	25% PANI/PbS	1.438	3.0096	29.650

Ultraviolet and visible (UV-Vis) spectroscopy of PANI/PbS nanocomposite

The most extreme assimilation frequency of unadulterated PbS and PANI/PbS nanocomposite are displayed in the (Fig. 4). In unadulterated PbS the retention frequency is getting at 263, 277 and 768 nm. It was interesting that the presence of retention groups at 400 to 500 nm in PANI/PbS nanocomposite were found. Because this band is absent from unadulterated PANI as well as unadulterated PbS. This fact demonstrated that when PbS nanoparticle collaborates with PANI some underlying change happened. The presence of this band in the nanocomposite gives the photoluminous qualities. The polaron-π*transition band at 320 to 385 nm turns out to be more extensive and shows the red shift. This infers that the doping condition of the nanocomposites has been moved along. Such peculiarities can be credited to the presence of more noteworthy number of charges on the polymer spine by bringing nanocrystalline PbS into the polymer matrix [16].

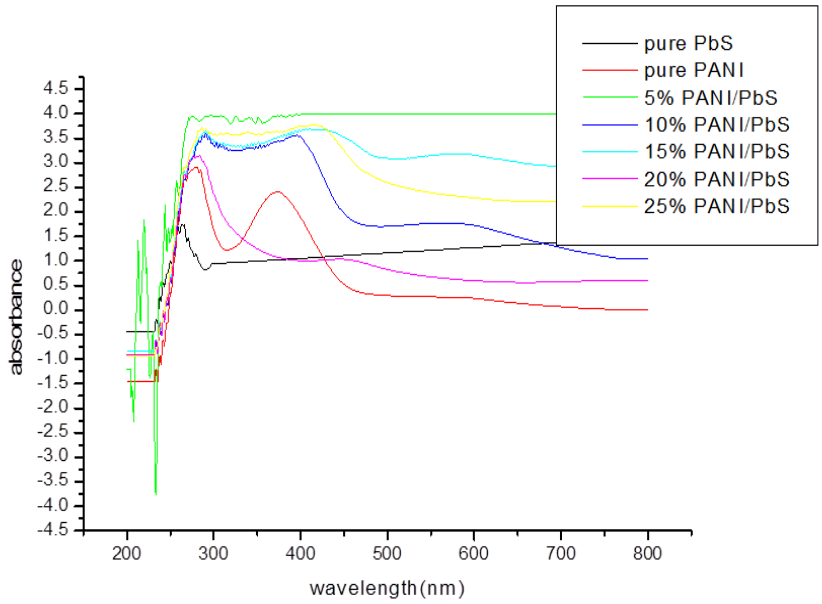

Fig. 4. UV–Vis absorption spectra of PbS/PANI nanocomposite at different wavelength

Fourier transforms infrared spectroscopy of PANI/PbS nanocomposite

Figure 5 shows FTIR spectra of pure polyaniline and PANI/PbS nanocomposites with different content (wt. %) of PbS. The incorporation of PbS nanoparticles caused the shift of some peaks of PANI and PbS. The absorption peak corresponds to polyaniline at 1566 shows red shift to 1561, 1557, 1516 and 1561 cm^{-1} respectively at 5%PbS, 10%PbS, 15%PbS, and 20%PbS nanocomposites. The absorption peak at 1485 showed a blue shift with respect to pure PANI peak, and they were moved to 1496, 1498, 1493 and 1495 cm^{-1} respectively at 5%PbS, 10%PbS, 15%PbS, and 20%PbS nanocomposites. Similarly, the peak at 1284, 1284, 1290 cm^{-1}, showed a blue shift with respect to pure PANI peak at 5, 10 and 20%PANI/PbS nanocomposites. But in 15%PANI/PbS nanocomposite the peak shows the blue shift as compared to pure PANI peak. The absorption peak at 1107 showed a blue shift with respect to pure PANI peak at 1179 cm^{-1}

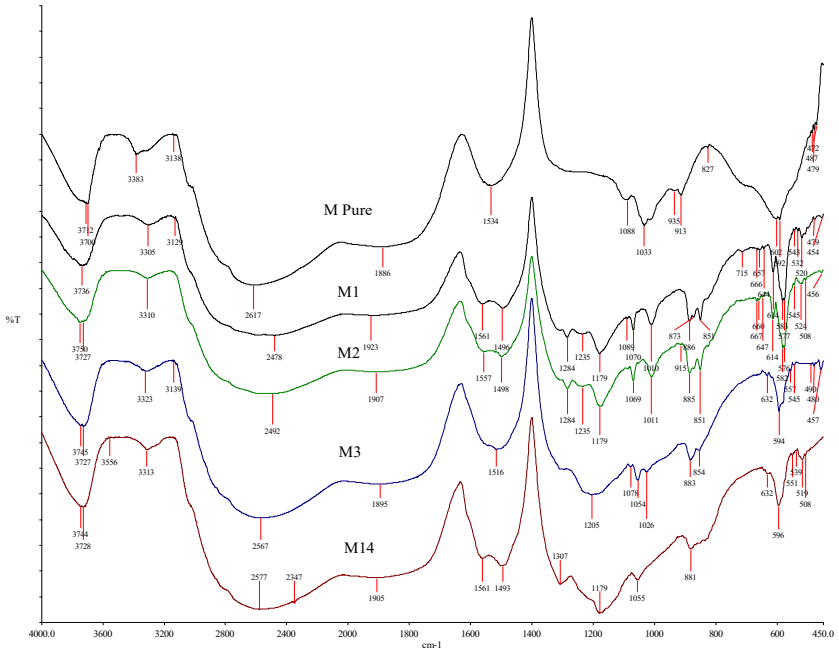

Fig. 5. FT-IR spectra of pure PANI and PANI/PbS nanocomposite

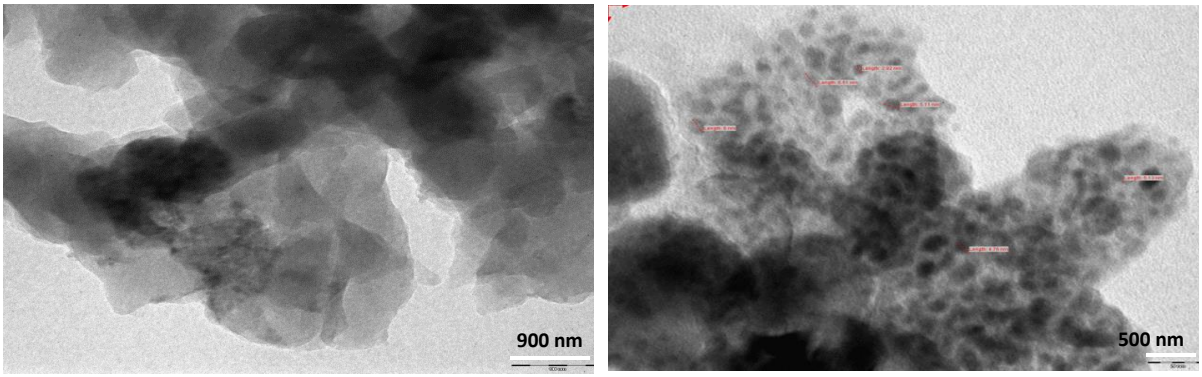

(a) (b)

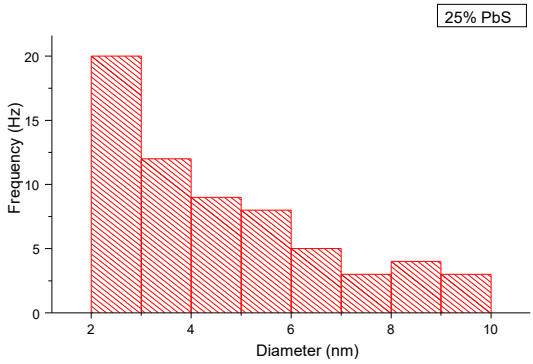

(c)

Fig. 6. TEM images of (a) pure PANI and (b) PANI/PbS nanocomposite, and average (c) diameter of particle size of nanocomposite

for 5, 10 and 20%PANI/PbS nanocomposites. PbS and PANI formed a coordination bond, and the electrons transferred from PANI to PbS which led to weakened bond strengths and the conjugated system of PANI and thus weakened vibration of PANI. The band in the

regions over 400 cm^{-1} can be assigned to PbS stretching vibrations FTIR spectra of the PANI/PbS nanocomposite are similar to those of PANI, but the bands' characteristic of polymer backbone at 1400 and 1500 cm^{-1} are shifted to higher values after annealing, indicating deprotonation. The peak at 1107 cm^{-1} is suppressed after annealing to a greater extent for PANI compared to that for the nanocomposites, indicating a higher extent of deprotonation in pure PANI compared to nanocomposites. The results of FTIR spectra confirm the presence of both components in the nanocomposite.

Transmission electron microscopy of PANI/Pbs nanocomposite

Transmission electron microscopy (TEM) images (Fig. 6) show the morphology of unadulterated PbS and PANI/PbS nanocomposite doped H_2SO_4. TEM image of (10 %) PANI/PbS nanocomposite (Fig. 6(b)) shows that particles were collected into a major construction, albeit the particles were in touch with one another. Most of the particles are comparative size and have unpredictable adjusted shapes. When content (wt. %) of PbS nanoparticle expanded in the polymer, then molecule size diminished (Fig. 6(c)). The nanocomposite turns out to be more arranged structure, consequently electrical conductivity is likewise expanded [29,30]. This is additionally clear by XRD and UV spectra. The typical distance across nanoparticles is 12 nm territory.

DTA analysis of pure PANI and PANI nanocompposite

Figure 7 shows DTA thermogram of PANI/PbS (5 to 25 %) nanocomposite, which showed just endothermic tops at around 230 to 245 °C because of the vanishing of water particles caught inside the composite or bound to the polymer spine. while the change above 350 °C might be alloted because of the corruption of composite. The diminished beginning worth of temperatures from 284 °C (unadulterated PANI) to 242.59, 244.15, 233.06, 227.55 and 237.25 °C for various wt. % of (5–25 %) PANI/PbS nanocomposite demonstrated that the warm steadiness of nanocomposite is greater than that of

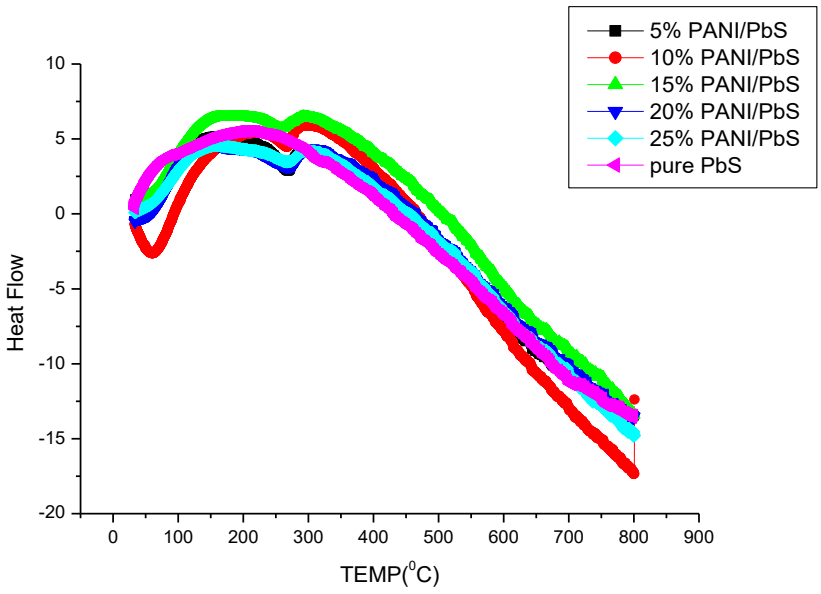

Fig. 7. The graph of differential thermal analysis of pure PbS and PANI/PbS (5–25%) nanocomposites

unadulterated PANI which could be credited to the impediment impact of nanostructures PbS as hindrances for the debasement of PANI [28–30]. In DTA of PANI the glass progress was not recognizable, in light of the fact that the glass change is covered in the top because of the evacuation of water and it doesn't display hysteresis. The exothermic progress at 99–160 °C is accepted not to be Tg. Rather it would be credited to a progression of compound responses. The diminished pinnacle temperatures of PANI/PbS nanocomposite, further show the arranged polymer structure as well as great interfacial communications between the metal oxide and the polymer grid. The DSC (differential scanning calorimetry) after-effects of composite materials are additionally found in great concurrence with TGA results which demonstrate that all the nanocomposites show least worth of beginning temperature as contrast with the unadulterated PANI.

Table 2 shows the data of warm boundary of Polyaniline nanocomposite with various content of PbS. Some changes in the softening temperature and enthalpy in PANI/PbS (5–25%) nanocomposite showed miscibility with PANI lattice.

Table 2. Thermal parameter of pure PANI and PANI/PbS nanocomposite

Sr. No	Material	Melting temp, °C	Onset temp. °C	Enthalpy change, J/g	Specific heat (ΔCp), J/g×°C	Peak area
1	Pure PANI	-	284.000	-	12.270	-
2	5%PANI/PbS	268.310	246.590	47.370	9.980	264.377
3	10%PANI/Pbs	267.880	244.150	34.460	6.520	167.613
4	15%PANI/PbS	266.810	240.060	30.479	6.479	123.622
5	20%PANI/PbS	265.130	232.550	28.699	5.192	125.700
6	25%PANI/PbS	263.420	230.250	26.861	4.405	120.234

Conclusions

XRD and UV-visible spectroscopy results indicated that the structural changes take place in nanocomposite with PbS nanoparticle. Thermal analysis of PbS nanocomposite indicated that the Polyaniline powder had discernible moisture content. This phenomenon is in agreement with the XRD results. Moreover, in the first run of DTA thermal analysis, an exothermic peak at 150–310 °C was found. This peak was due to the chain cross linking, resulting from a coupling of two neighboring -N=Q=N- groups to give two -NH-B-NH groups through a link of the N with its neighboring Quindío ring. Thus, based on the thermal profile of these materials, we can say that among all composite material, the PANI/PbS composite materials, cross-linking or oxidative reaction starts at higher temperature than other composites, which indicates that the thermal stability of PANI/PbS nanocomposites is higher than oxides nanocomposites. These DTA results of composite materials are also found in good agreement with XRD results.

CRediT authorship contribution statement

Jitendra Bhaiswar, Meghe Dhiraj: writing original draft and investigation, review and editing; **Dongre Sunil** Sc: supervision of draft and conceptualization.

Conflict of interest

The authors declare that they have no conflict of interest.

References

1. Maziarz EP, Lorenz SA, White TP, Wood TD. Polyaniline: A conductive polymer coating for durable nanospray emitters. *J Am Soc Mass Spectrom*. 2000;11: 659–663.
2. Tiitu M, Talo A, Forsén O, Ikkala O. Aminic Epoxy Resin Hardeners as Reactive Solvents for Conjugated Polymers: Polyaniline Base/Epoxy Composites for Anticorrosion Coatings. *Polymer*. 2005;46(18): 6855–6861.
3. Ismail YA, Shin SR, Shin KM, Yoon SG, Shon K, Kim SI, Kim SJ. Electrochemical Actuation in Chitosan/Polyaniline Microfibers for Artificial Muscles Fabricated using an in Situ Polymerization. *Sensors and Actuators B: Chemical*. 2008;129(2): 834–840.
4. Dhand C, Das M, Sumana G, Srivastava AK, Pandey MK, Kim CG, Datta M, Malhotra BD. Preparation, Characterization and Application of PolyanilineNanospheres to Biosensing. *Nanoscale*. 2010;2: 747–754.
5. Saxena V, Malhotra BD. Prospects of Conducting Polymers in Molecular Electronics. *Current Applied Physics*. 2003;3(2–3): 293–305.
6. Pinto N, Johnson A, MacDiarmid A, Mueller C, Theofylaktos N, Robinson D, Miranda F. Electrospun Polyaniline/Polyethylene Oxide Nanofiber Field-Effect Transistor. *Applied Physics Letters*. 2003;83(20): 4244–4246.
7. Tan S, Zhai J, Xue B, Wan M, Meng Q, Li Y, Jiang L, Zhu D. Property Influence of Polyaniline on Photovoltaic Behaviors of Dye-Sensitized Solar Cells. *Langmuir*. 2004;20(7): 2934–2937.
8. Hosseini SH, Oskooei SHA, Entezami AA. Toxic Gas and Vapour Detection by Polyaniline Gas Sensors. *Iranian Polymer Journal*. 2005;14(4): 333–344.
9. Sadek AZ, W Wlodarski, Kalantar-Zadeh K, Baker C, Kaner RB. Doped and dedoped polyaniline nanofiber based conductometric hydrogen gas sensors. *Sensors and Actuators A: Physical*. 2007;139(1–2): 53–57.
10. Matsunaga T, Daifuku H, Nakajima T, Kawagoe T. Development of polyaniline–lithium secondary battery. *Polymers for Advanced Technologies*. 1990;1(1): 33–39.
11. Wang H, Hao Q, Yang X, Lu L, Wang X. Graphene oxide doped polyaniline for supercapacitors. *Electrochemistry Communications*. 2009;11(6): 1158–1161.
12. Kovalenko I, Bucknall DG, Yushin G. Detonation nanodiamond and onion-like-carbon-embedded polyaniline for supercapacitors. *Advanced Functional Materials*. 2010;20(22): 3979–3986.
13. X Huang, G Wang, M Yang, W Guo, H Gao. Synthesis of polyaniline-modified Fe3O4/SiO2/TiO2 composite microspheres and their photocatalytic application. *Materials Letters*. 2011;65(19–20): 2887–2890.
14. Heera TR, Cindrella L. PbS/CoS–Pani composite semiconductor films. *Materials Science in Semiconductor Processing*. 2011;14(2): 151–156.
15. Li Q, Zhang C, Li J. Photocatalysis and Wave-Absorbing Properties of Polyaniline/TiO2 Microbelts Composite by in Situ Polymerization Method. *Applied Surface Science*. 2010;257(3): 944–948.
16. Wang Y, Herron N. Semiconductor Nanocrystals in Carrier-Transporting Polymers: Charge Generation and Charge Transport. *Journal of Luminescence*. 1996;70(1–6): 48–59.
17. Liu XX, Zhang L, Li YB, Bian LJ, Huo YQ, Su Z. Electrosynthesis of Polyaniline/SiO2 Composite at High pH in the Absence of Extra Supporting Electrolyte. *Polymer Bulletin*. 2006;57: 825–832.
18. Pulin AG, Laptev MA, Alisov KA, Barskov VV, Rassokhin VA, Gong B, Kotov VS, Roshchenko GA, Balakin AM, Golubtsov M, Nurkov IR, Basati Panah M. Heat exchanger and the influence of lattice structures on its strength. *Materials Physics and Mechanics*. 2024;52(6): 61–80.
19. Kaminskii VV, Panov DYu, Spiridonov VA, Bauman DA, Kalganov DA, Scheglov MP, Romanov AE. Effect of high-temperature annealing on the internal friction and optical transmittance of single crystal gallium oxide. *Materials Physics and Mechanics*. 2024;52(5): 48–54.
20. Pozdnyakov AO, Sedakova EB. Thermal analysis of wear of polymer-polymer friction pairs in vacuum and atmosphere conditions. *Materials Physics and Mechanics*. 2024;52(4): 63–80.
21. Arena A, Taló M, Snyder MP, Lacarbonara W. Enhancing flutter stability in nanocomposite thin panels by harnessing CNT/polymer dissipation. *Mech. Res. Commun*. 2020;104: 103495.
22. Xia X, Du Z, Zhang J, Li J, Weng GJ. Modeling the impact of glass transition on the frequency-dependent complex conductivity of CNT-polymer nanocomposites. *Mech. Mater*. 2022;165: 104195.

23. Patnaik SS, Roy T. Viscoelastic and mechanical properties of CNT-reinforced polymer-based hybrid composite materials using hygrothermal creep. *Polym. Polym. Compos.* 2021;29(9): 1386–1402.
24. Ma Q, Hao B, Ma PC. In-situ characterization on the fracture behavior of three dimensional polymer nanocomposites re-inforced by CNT sponge. *Compos. Sci. Technol.* 2022;217: 109132.
25. Anwer AH, Ahtesham A, Shoeb M, Mashkoor F, Ansari MZ, Zhu S, Jeong C. State-of-the-art advances in nanocomposite and bio-nanocomposite polymeric materials: a comprehensive review. *Adv. Colloid Interface Sci.* 2023;318: 102955.
26. Jagadeesh N, Sundaram B. Adsorption of pollutants from wastewater by biochar: a review. *J. Hazard. Mater. Adv.* 2023;9: 100226.
27. Naz S, Gul A, Zia M, Javed R. Synthesis, biomedical applications, and toxicity of CuO nanoparticles. *Appl. Microbiol. Biotechnol.* 2023;107(4): 1039–1061.
28. Mei Y, Shen Z, Kundu S, Dennis E, Pang S, Tan F, Yue G, Gao Y, Dong C, Liu R, Zhang W, Saidaminov MI. Perovskite solar cells with polyaniline hole transport layers surpassing a 20% power conversion efficiency. *Chem Mater.* 2021;33(12): 4679–4687.
29. Deyab MA, Mele G, Bloise E, Mohsen Q. Novel nanocomposites of Ni-pc/polyaniline for the corrosion safety of the aluminum current collector in the Li-ion battery electrolyte. *Sci Rep.* 2021;11(1): 1–8.
30. Zhang X, Wang Y, Fu D, Wang G, Wei H, Ma N. Photo-thermal converting polyaniline/ionic liquid inks for screen printing highly-sensitive flexible uncontacted thermal sensors. *Eur Polym J.* 2021;147: 110305.